

On the computation of structure factors by FFT techniques

Jorge Navaza

CNRS-GIF, LGV, 91198 Gif-sur-Yvette, France. Correspondence e-mail: jnavaza@pasteur.fr

The method of structure-factor calculation by fast Fourier transform techniques [Ten Eyck (1977). *Acta Cryst.* **A33**, 486–492] is here reviewed. It is found that the recommended sampling of three times the highest index in each direction [Lipson & Cochran (1966). *The Determination of Crystal Structures*, 3rd ed., pp. 94–102. Ithaca: Cornell University Press] is appropriate for any resolution, provided an adequate Gaussian dampening factor is used. A rule is given to determine this factor.

© 2002 International Union of Crystallography
 Printed in Great Britain – all rights reserved

1. Introduction

In Ten Eyck's (1977) method for structure-factor calculation, the Fourier transform of a model electron density is computed using the fast Fourier transform algorithm (FFT). The model electron density is the sum of atomic contributions obtained by transforming the atomic scattering factors, usually expressed as a sum of Gaussians. The atomic contributions can then be recovered analytically and their values used to compute the model electron density on a grid, which poses the problem of sampling. This problem is solved by using a result of Brillouin (1956), which relates the Fourier coefficients, $F(H)$, H integer, of a periodic function of period a with those, $C(H)$, obtained by computing the discrete Fourier transform of the function sampled at N equidistant points spaced out by a/N :

$$C(H) = \sum_{n=-\infty}^{\infty} F(H + nN). \quad (1)$$

If the contribution of the $n \neq 0$ terms is negligible, then $C(H)$ is close to $F(H)$. This is not in general the case for reasonable values of N . The procedure proposed by Ten Eyck (1977) to solve this problem consists in adding an *ad hoc* thermal parameter B to all the atomic temperature factors. Then, $F(H)$ becomes $F(H) \exp(-\frac{1}{4}BH^2/a^2)$ and (1) becomes

$$C_B(H) = \sum_{n=-\infty}^{\infty} F(H + nN) \exp[-\frac{1}{4}B(H + nN)^2/a^2]. \quad (2)$$

This gives, after multiplication by $\exp(+\frac{1}{4}BH^2/a^2)$,

$$C_B(H) \exp(\frac{1}{4}BH^2/a^2) = F(H) + \sum_{n \neq 0} F(H + nN) \times \exp[-\frac{1}{4}BnN(nN + 2H)/a^2]. \quad (3)$$

Since $2|H| < N$, as required by the discrete Fourier transform algorithm, an appropriate choice of N and B can render the exponentials in the right-hand member arbitrarily small, the left-hand member thus approaching $F(H)$. To summarize: the atomic scattering factors are first multiplied by a Gaussian and the resulting atomic electron densities are used to sample the

model density on a grid. This is fast Fourier transformed and the calculated structure factors are divided by the Gaussian.

However, no rule to determine B or N was proposed. The main result of this article is the establishment of such a rule.

2. Model electron density

The atomic scattering factor is usually given by a linear combination of four Gaussians plus a constant term (Doyle & Turner, 1968), which we write as

$$f_{\text{atom}}(|\mathbf{s}|) = \sum_{n=0}^4 a_n \exp(-\frac{1}{4}b_n \mathbf{s}^2) \quad (4)$$

with $b_0 = 0$. \mathbf{s} is the scattering vector of resolution $1/|\mathbf{s}|$. The values of the coefficients a_n, b_n for free atoms or ions are compiled in *International Tables for Crystallography* (1992), Vol. C. The values of b_n present a great dispersion (see Fig. 1), ranging from 0 to 214 for neutral atoms. The atomic electron density is then a linear combination of Gaussians obtained by analytical transformation of (4),

$$\rho_{\text{atom}}(|\mathbf{r}|) = \sum_{n=0}^4 a_n (4\pi/b_n)^{3/2} \exp[-\frac{1}{2}(8\pi^2/b_n)\mathbf{r}^2], \quad (5)$$

and the model electron density

$$\rho(\mathbf{r}) = \sum_{\text{atom}} \rho_{\text{atom}}(|\mathbf{r} - \mathbf{r}_{\text{atom}}|), \quad (6)$$

where \mathbf{r}_{atom} denotes an atomic position. The sum is taken over the atoms in the unit cell. The advantage of (4) and (5) is that they keep their forms after incorporating the atomic (isotropic) temperature factors, B_{iso} , and the thermal parameter B . Indeed, this amounts to substituting b_n by $b_n + B_{\text{iso}} + B$ in these equations.

The structure factors may be calculated either by direct summation

$$F(\mathbf{s}) = \sum_{\text{atom}} f_{\text{atom}}(|\mathbf{s}|) \exp(2\pi i \mathbf{s} \cdot \mathbf{r}_{\text{atom}}) \quad (7)$$

or by numerical integration of

$$F(\mathbf{s}) = \int \rho(\mathbf{r}) \exp(2\pi i \mathbf{s} \cdot \mathbf{r}) d^3 \mathbf{r}. \quad (8)$$

The last approach poses the problem of sampling of ρ . According to (5) and (6), this can be reduced to the case of a single Gaussian. In the following two sections, we will investigate the problem of sampling in one dimension.

3. Sampling of a Gaussian

We want to assess the error made when computing the Fourier transform of a Gaussian

$$\frac{1}{\sigma(2\pi)^{1/2}} \int_{-\infty}^{\infty} \exp(-\frac{1}{2}x^2/\sigma^2) \exp(2\pi i s x) dx = \exp[-\frac{1}{2}(2\pi\sigma s)^2] = G(\sigma s) \quad (9)$$

by means of a discrete summation. The root-mean-square deviation parameter, σ , is related to the temperature B factor by the relationship

$$\sigma = (B/8\pi^2)^{1/2}. \quad (10)$$

We first divide the x axis into steps of width Δ and perform the substitutions

$$dx \rightarrow \Delta; \quad x \rightarrow j\Delta \quad (11)$$

(j integer) in the right-hand member of (9), obtaining

$$C(s) = \frac{\Delta}{\sigma(2\pi)^{1/2}} \sum_{j=-\infty}^{\infty} \exp[-\frac{1}{2}(j\Delta)^2/\sigma^2] \exp(2\pi i s j\Delta). \quad (12)$$

Brillouin's result [equation (1)] generalized to Fourier integrals (a proof is given in Appendix A) gives

$$C(s) = \sum_{n=-\infty}^{\infty} \exp[-\frac{1}{2}(2\pi\sigma)^2(s + n/\Delta)^2] = \sum_{n=-\infty}^{\infty} \exp[-\frac{1}{2}(2\pi\sigma/\Delta)^2(s\Delta + n)^2]. \quad (13)$$

We note that the pertinent variables are the dimensionless quantities

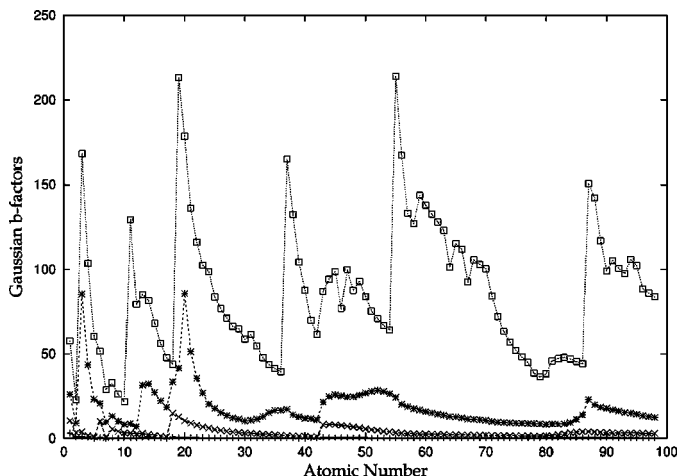


Figure 1 Coefficients b_n of the 4-Gaussians-plus-constant fit of the atomic scattering factors, for neutral atoms, as a function of the atomic number.

$$s' = s\Delta; \quad \sigma' = \sigma/\Delta. \quad (14)$$

It follows that $G(\sigma s) = G(\sigma' s')$.

The theoretical relative error made when computing the discrete sum instead of the integral is

$$\begin{aligned} \mathcal{E}^{(\text{theory})}(\sigma', s') &= |1 - C(s)/G(\sigma' s')| \\ &= \sum_{n \neq 0} \exp\{-\frac{1}{2}(2\pi\sigma')^2[(s' + n)^2 - s'^2]\} \\ &= \sum_{n \neq 0} \exp[-\frac{1}{2}(2\pi\sigma')^2 n(n + 2s')]. \end{aligned} \quad (15)$$

$\mathcal{E}^{(\text{theory})}$ is an even function of s' ; we will only consider the region $s' \geq 0$. It can be readily shown that

$$\partial \mathcal{E}^{(\text{theory})} / \partial \sigma' < 0; \quad \partial \mathcal{E}^{(\text{theory})} / \partial s' > 0. \quad (16)$$

These inequalities imply that a curve of constant $\mathcal{E}^{(\text{theory})}$ defines s' as an increasing function of σ' .

The center of the Gaussian may not coincide with a sampling point [$j = 0$ in (12)] but lie somewhere within the interval Δ . Its position may be written as $\zeta\Delta$, with $0 \leq \zeta \leq 1$. The only change in (15) is that each term of the series is now multiplied by $\exp(2\pi i \zeta n)$. The sum of their moduli is then the same, so (15) is an upper bound of the relative error for any position of the Gaussian.

In practice, $C(s)$ is computed using a finite number of sampling points. The experimental (numerical) relative error of the discrete approximation is then

$$\begin{aligned} \mathcal{E}^{(\text{calc})}(\sigma', s', J) &= \left| 1 - \frac{\exp[\frac{1}{2}(2\pi\sigma' s')^2]}{\sigma'(2\pi)^{1/2}} \right. \\ &\quad \left. \times \sum_{j=-J}^J \exp(-\frac{1}{2}j^2/\sigma'^2) \exp(2\pi i s' j) \right|. \end{aligned} \quad (17)$$

The cutoff J , hence the number of sampling points, depends on the cutoff for the Gaussian contributions. For example, if

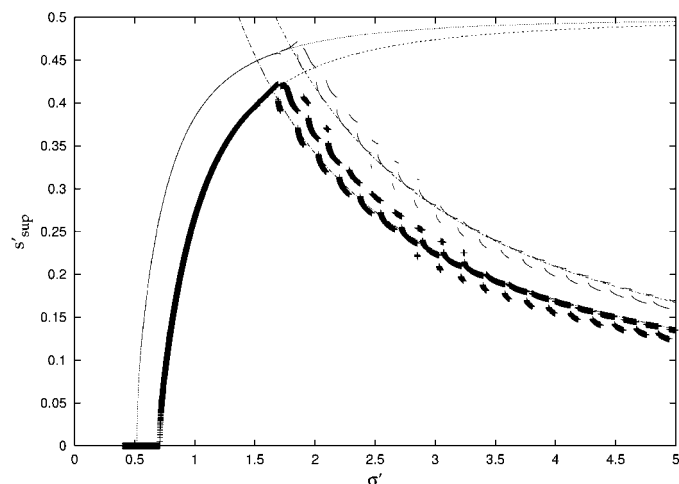


Figure 2 Upper limit of the scattering vectors, s'_{sup} , as a function of σ' , for a Gaussian cutoff of 10^{-6} and two values of the maximum relative error, $\mathcal{E}^{(\text{calc})} = 10^{-p}$, $p = 4, 2$. The discontinuities are produced by round-off errors. The increasing continuous curves correspond to $\mathcal{E}^{(\text{theory})}(\sigma', s') = 10^{-p}$, $p = 4, 2$ and the decreasing ones to $G(\sigma' s') = 10^{-p}$, $p = 4, 6$.

we want to keep only terms greater than 10^{-p} , *i.e.* $\exp(-\frac{1}{2}j^2/\sigma^2) \geq 10^{-p}$, then the sum must be taken over the integers that satisfy

$$|j| \leq J \approx \sigma'[\ln(100)p]^{1/2}. \quad (18)$$

It is important to identify the values of (σ', s', J) that make $\mathcal{E}^{(\text{calc})}$ smaller than a prescribed (attainable) value. It is found that, for fixed σ' and Gaussian cutoff, hence J , the inequality is satisfied by all s' smaller than a maximum value s'_{sup} , *i.e.*

$$\mathcal{E}^{(\text{calc})}(\sigma', s', J) \leq \varepsilon \quad \text{for } 0 \leq s' \leq s'_{\text{sup}}(\sigma', J, \varepsilon), \quad (19)$$

as shown in Fig. 2. As long as the value of $G(\sigma's')$ is higher than a certain limit related to ε and the Gaussian cutoff, $\mathcal{E}^{(\text{calc})}$ approximates quite well the corresponding theoretical value $\mathcal{E}^{(\text{theory})}$. This can be readily seen by plotting $G(\sigma's'_{\text{sup}})$ as a function of σ' , as shown in Fig. 3. A similar plot is shown in Fig. 4 for fixed maximum relative error and different Gaussian cutoffs. The computations were performed in double precision (real**8) and using the Fortran compiler built-in functions exp, sin, cos. It is known that round-off errors are then somewhat greater than when using the FFT algorithm.

4. Structure-factor calculation

What is given in practice is the cell parameter a , which is also the periodicity of the model electron density, and the coefficients of the Gaussian. One has to determine the number of sampling points N or, equivalently, the spacing $\Delta = a/N$. According to (17) and (18), the effective number of sampling points for each particular Gaussian is $2J + 1$. N is usually greater than the maximum $2J$.

Structure factors are usually computed up to a given resolution d_{min} , related to a maximum Miller index H_{max} ,

$$|s| \leq 1/d_{\text{min}} = s_{\text{max}}; \quad H_{\text{max}} = a/d_{\text{min}}. \quad (20)$$

The FFT algorithm requires that $2H_{\text{max}} + 1 \leq N$. The quotient between the actual and the minimum allowed number of

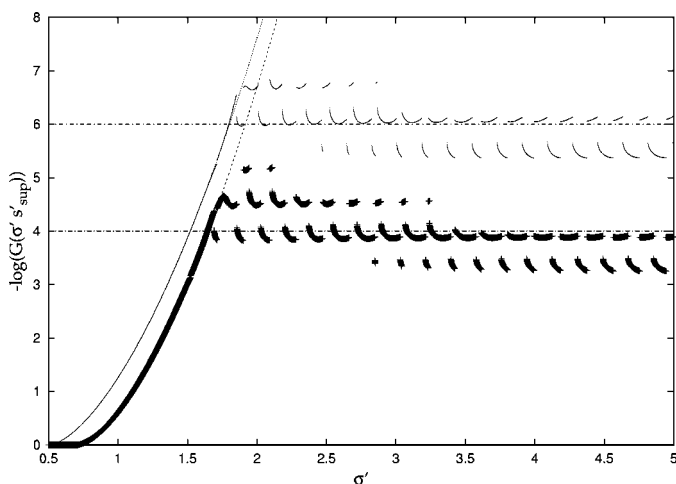


Figure 3
Values of $G(\sigma's'_{\text{sup}})$, in minus logarithmic scale, versus σ' , for the calculations shown in Fig. 2. The continuous curves correspond to the theoretical values. The horizontal lines are drawn for reference.

sampling points is called the Shannon rate. We shall define it as

$$R = N/2H_{\text{max}} > 1. \quad (21)$$

The smaller is R , the more economic is the computation. For example, the Lipson & Cochran (1966) prescription is $R = 1.5$. The maximum (dimensionless) length of the reciprocal vectors whose structure factors have to be calculated is simply half the inverse of the Shannon rate

$$s'_{\text{max}} = s_{\text{max}}\Delta = (1/d_{\text{min}})(a/N) = H_{\text{max}}/N = 1/2R. \quad (22)$$

If the atomic scattering factors are represented by a unique Gaussian of coefficient b , or a constant term in the case of point atoms ($b = 0$), and all atoms have the same temperature factor B_{iso} , then Fig. 2 suggests that the best choice of s'_{max} is the highest value (the smallest Shannon rate) compatible with a chosen maximum relative error and Gaussian cutoff. The associated σ'_{min} is determined using the corresponding curve of Fig. 2. For a maximum relative error of 10^{-4} and Gaussian cutoff of 10^{-6} , $s'_{\text{max}} = 0.4$ and $\sigma'_{\text{min}} \approx 1.527$. This corresponds to the rather small Shannon rate $R = 1.25$. However, we must also satisfy $N > 2J$. Using (18) and the preceding equations, we have

$$N = (a/d_{\text{min}})1/s'_{\text{max}} > 2\sigma'_{\text{min}}[\ln(100)p]^{1/2} \quad (23)$$

or

$$\sigma'_{\text{min}}s'_{\text{max}} < (a/d_{\text{min}})/\{2[\ln(100)p]^{1/2}\}. \quad (24)$$

This gives, with the above values, $a/d_{\text{min}} > 6.42$. If the inequality is not satisfied by the desired d_{min} , a smaller s'_{max} must be chosen, and its associated σ'_{min} , using Fig. 2 and Fig. 3. With these values, N and B are obtained as functions of a , d_{min} and $b + B_{\text{iso}}$

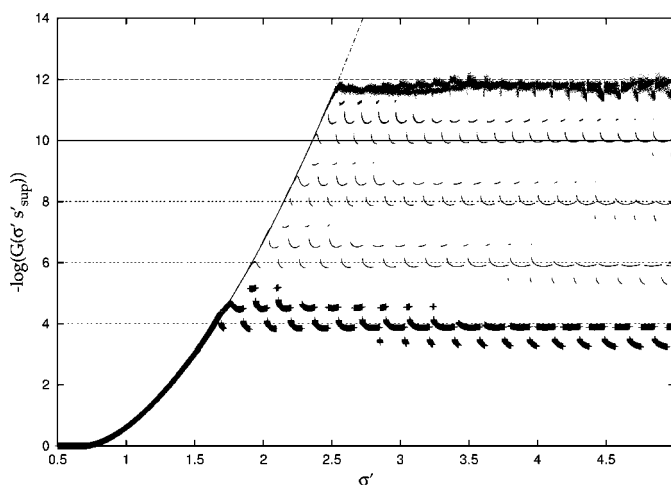


Figure 4
Values of $G(\sigma's'_{\text{sup}})$, in minus logarithmic scale, versus σ' , for different Gaussian cutoffs, 10^{-p} , $p = 6, 8, 10, 12, 14$, and a maximum relative error of 10^{-4} . The continuous curve corresponds to the theoretical values. The horizontal lines are drawn for reference.

$$\begin{aligned}
 N &= (a/d_{\min})1/s'_{\max} \\
 \sigma_{\min} &= \sigma'_{\min} \Delta = \sigma'_{\min} s'_{\max} d_{\min} \\
 b_{\min} &= b + B_{\text{iso}} \\
 B &= 8\pi^2 \sigma_{\min}^2 - b_{\min}.
 \end{aligned}
 \quad (25)$$

In practice, not only each atom has its individual B_{iso} but also the atomic scattering factors are given by a sum of Gaussians [equation (4)]. We may substitute b_{\min} in (25) by the minimum of $b_n + B_{\text{iso}}$ over the set of all atoms. For neutral atoms, this is simply the minimum atomic B_{iso} because of the $b_0 = 0$ term in (4). But now we must check that all Gaussians contribute with an acceptable error.

From Fig. 2, we see that the smaller is the resolution, the wider is the range of allowed σ' . Given the great dispersion of the atomic b_n and B_{iso} , it is almost impossible to keep the relative error of each contribution below a desired value. However, the absolute error is roughly constant beyond the upper limit of the allowed σ' region. This is because a rise in relative error is compensated by a fall in contribution; the drop in absolute error is thus proportional to the drop in contribution.

It is then natural to choose σ'_{\min} as the minimum allowed value for a chosen maximum relative error $\mathcal{E}^{(\text{theory})}$ at the highest resolution s'_{\max} . It helps to read Fig. 2 in a different way: $G(\sigma's')$ versus $(2s')^{-1}$ (Fig. 5). Now we can directly observe, for fixed resolution, the drop in contribution between the lower and the upper limits of the allowed σ' region. With $(2s'_{\max})^{-1} = R = 1.5$, there is a drop of more than two orders of magnitude. Little is gained beyond $R = 2$. The drop may be increased by decreasing the Gaussian cutoff, as shown in Fig. 4.

In summary, the rule to determine N and B is:

(i) get b_{\min} , the minimum of $b_n + B_{\text{iso}}$ over the set of all atoms;

(ii) select the Shannon rate $R = (2s_{\max})^{-1}$ from Fig. 5 such that the drop in Gaussian contribution at the farthest limit of

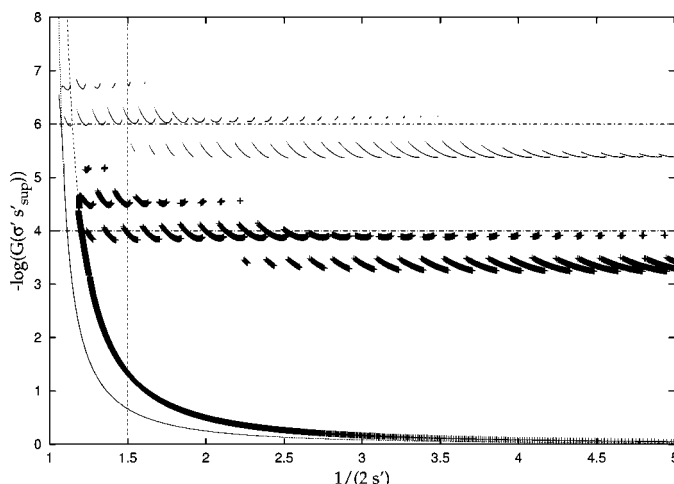


Figure 5
Values of $G(\sigma's'_{\text{sup}})$, in minus logarithmic scale, versus $1/(2s')$, for the calculations shown in Fig. 2. The continuous curves correspond to the theoretical values. The abscissas can also be interpreted as Shannon rates. The vertical line shows the points that correspond to a Shannon rate of 1.5.

the allowed region for that R is of the desired order of magnitude;

(iii) get the σ'_{\min} corresponding to the selected value of $R = (2s'_{\max})^{-1}$ from Fig. 2. Check that inequality (24) is satisfied;

(iv) determine N and B using (25).

The structure-factor calculation is then performed following Ten Eyck's (1977) method as recalled in the *Introduction*.

5. The three-dimensional case

The results obtained in the preceding section can be readily adapted to the real case of molecular scattering factor and crystal structure-factor calculations. Now we have

$$(2\pi\sigma^2)^{-3/2} \int \exp(-\frac{1}{2}\mathbf{r}^2/\sigma^2) \exp(2\pi i \mathbf{s} \cdot \mathbf{r}) d^3 \mathbf{r} = \exp[-\frac{1}{2}(2\pi\sigma\mathbf{s})^2],
 \quad (26)$$

and its discrete form version (see Appendix A)

$$\begin{aligned}
 c(\mathbf{s}) &= \frac{\Delta_x \Delta_y \Delta_z}{(2\pi\sigma^2)^{3/2}} \sum_{j_1, j_2, j_3 = -\infty}^{\infty} \exp[-\frac{1}{2}(j_1 \Delta_x \mathbf{a} + j_2 \Delta_y \mathbf{b} + j_3 \Delta_z \mathbf{c})^2 / \sigma^2] \\
 &\quad \times \exp[2\pi i (j_1 \Delta_x \mathbf{s} \cdot \mathbf{a} + j_2 \Delta_y \mathbf{s} \cdot \mathbf{b} + j_3 \Delta_z \mathbf{s} \cdot \mathbf{c})] \\
 &= \sum_{n_1, n_2, n_3 = -\infty}^{\infty} \exp\left[-\frac{1}{2}(2\pi\sigma)^2 \left(\mathbf{s} + \frac{n_1}{\Delta_x} \mathbf{a}^* + \frac{n_2}{\Delta_y} \mathbf{b}^* + \frac{n_3}{\Delta_z} \mathbf{c}^*\right)^2\right]
 \end{aligned}
 \quad (27)$$

where $\{\Delta_x, \Delta_y, \Delta_z\}$ are the step widths along the cell axes $\{\mathbf{a}, \mathbf{b}, \mathbf{c}\}$. The Gaussian cutoff, *i.e.* $\exp(-\frac{1}{2}\mathbf{r}^2/\sigma^2) \geq 10^{-p}$, restricts the sum to the points within the sphere of radius $\sigma[\ln(100)p]^{1/2}$. For molecular scattering-factor calculation, *i.e.* Fourier coefficients corresponding to an isolated molecule, this sphere must fit into the unit cell. The step widths are simply the inverse of the number of sampling points in each direction,

$$(\Delta_x, \Delta_y, \Delta_z) = \left(\frac{1}{N_1}, \frac{1}{N_2}, \frac{1}{N_3}\right).
 \quad (28)$$

The relative error is given by

$$\begin{aligned}
 \mathcal{E}^{(\text{theory})}(\sigma, \mathbf{s}) &= |1 - c(\mathbf{s}) / \exp[-\frac{1}{2}(2\pi\sigma\mathbf{s})^2]| \\
 &= \sum_{(n_1, n_2, n_3) \neq (0,0,0)} \exp\{-\frac{1}{2}(2\pi\sigma)^2 (n_1 N_1 \mathbf{a}^* + n_2 N_2 \mathbf{b}^* \\
 &\quad + n_3 N_3 \mathbf{c}^*) [(n_1 N_1 \mathbf{a}^* + n_2 N_2 \mathbf{b}^* + n_3 N_3 \mathbf{c}^*) + 2\mathbf{s}]\}.
 \end{aligned}
 \quad (29)$$

Using a single Shannon rate, we substitute here the number of sampling points by

$$(N_1, N_2, N_3) = (a, b, c)2R/d_{\min},
 \quad (30)$$

taking for example the nearest integer of the right-hand term, and calculate the minimum σ that satisfies $\mathcal{E}^{(\text{theory})}(\sigma, \mathbf{s}) = \varepsilon$ for all $|\mathbf{s}| \leq 1/d_{\min}$. In practice, it suffices to take a small number of \mathbf{s} vectors, those with length $1/d_{\min}$ in the direction of

$$n_1 N_1 \mathbf{a}^* + n_2 N_2 \mathbf{b}^* + n_3 N_3 \mathbf{c}^*,
 \quad (31)$$

with n_1, n_2, n_3 taking values $-1, 0, 1$, excluding $(n_1, n_2, n_3) = (0, 0, 0)$. The sum in (29) may also be restricted to the same set of integers. Having σ_{\min} , we may obtain the B of the dampening factor using the last of equations (25), with b_{\min} equal to the minimum of $b_n + B_{\text{iso}}$ over the set of all atoms.

We applied the preceding rule to calculate structure factors for VP6, the major capsid protein of *Rotavirus* (Mathieu *et al.*, 2001), which crystallizes in the cubic space group $P4_132$ with a unit-cell constant of 157.78 \AA and only one monomer (3166 non-Hydrogen atoms) of the trimeric molecule in the asymmetric unit. The computations were performed in single precision (real**4) using subroutines of the *AMoRe* package (Navaza, 1994), which uses the kernel of Ten Eyck's FFT program (Ten Eyck, 1977). The Gaussian cutoff was set to

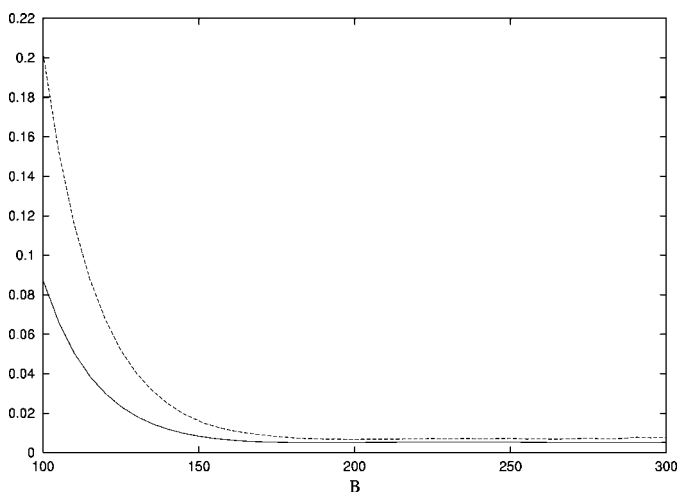


Figure 6 Crystal structure factors of VP6 calculated up to 4.5 \AA resolution using a Shannon rate of 1.5 and a Gaussian cutoff of 10^{-5} . R factor (lower curve) and average percent relative error, $100 \times \langle |F_{\text{calc}} - F_{\text{theory}}| / |F_{\text{theory}}| \rangle$, as a function of B . The estimated optimal B factor, solution of $\mathcal{E}^{(\text{theory})} = 10^{-3.5}$ [equation (29)], is 195 \AA^2 .

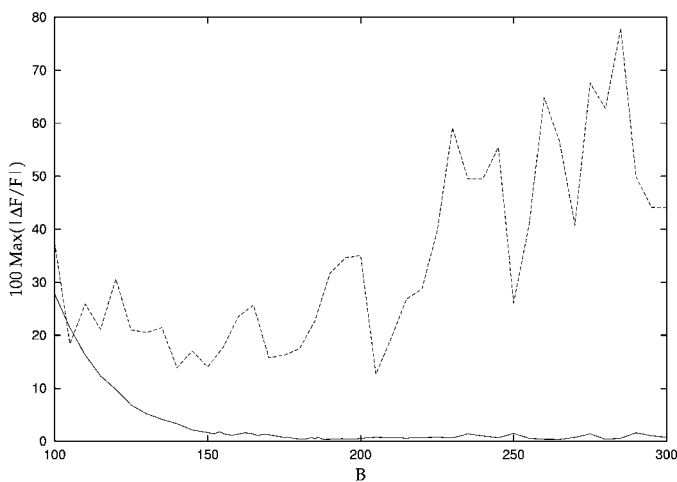


Figure 7 Maximum percent relative error, $100 \times \max(|F_{\text{calc}} - F_{\text{theory}}| / |F_{\text{theory}}|)$, of the calculated structure factors as a function of B for two different Gaussian cutoffs, $e^{-7} = 10^{-3.04}$ (overall upper curve) and 10^{-5} . Same test case as in Fig. 6.

10^{-5} . The 'exact' values of the Fourier coefficients were computed by direct summation [equation (7)].

In a first test, crystal data were calculated to 4.5 \AA resolution (4347 independent reflections) using a Shannon rate equal to 1.5, which gives a grid spacing of 1.5 \AA . The results for different B factors are shown in Figs. 6 and 7. The last figure also shows how critical the choice of a reasonable Gaussian cutoff is. For example, very poor results are obtained when the Gaussian contributions are restricted to values greater than the often used limit of $e^{-7} = 10^{-3.04}$. For the dampening factor $B = 195 \text{ \AA}^2$, which corresponds to $\mathcal{E}^{(\text{theory})} = 10^{-3.5}$ [equation (29)], the average relative error of the calculated complex structure factors is 0.0068% and the average phase error is 0.0011° .

In a second test, the molecular scattering factors were calculated up to 15 \AA , a typical calculation when fitting X-ray

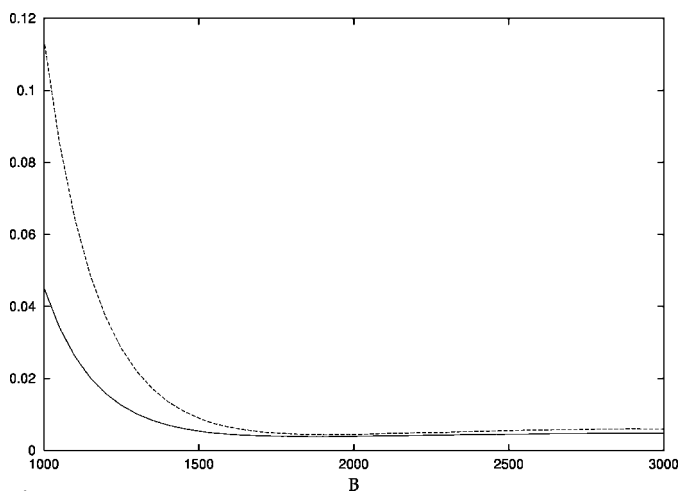


Figure 8 Molecular scattering factors of VP6 calculated up to 15 \AA resolution using a Shannon rate of 1.5 and a Gaussian cutoff of 10^{-5} . R factor (lower curve) and average percent relative error, $100 \times \langle |F_{\text{calc}} - F_{\text{theory}}| / |F_{\text{theory}}| \rangle$, as a function of B . The estimated optimal B factor ($\mathcal{E}^{(\text{theory})} = 10^{-3.5}$) is 1875 \AA^2 .

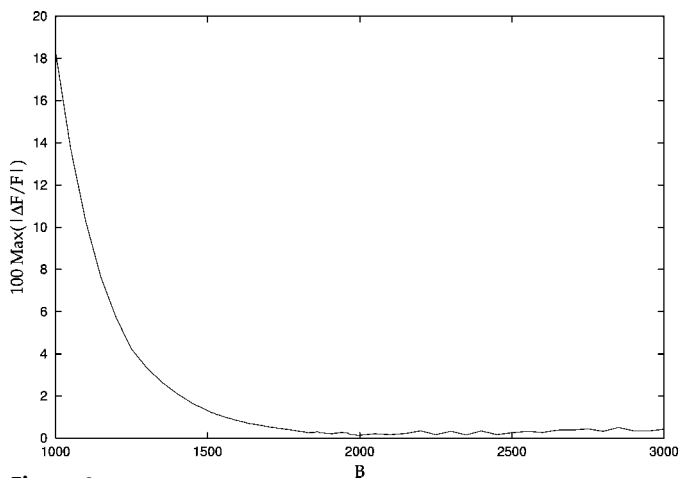


Figure 9 Maximum percent relative error, $100 \times \max(|F_{\text{calc}} - F_{\text{theory}}| / |F_{\text{theory}}|)$, of the calculated molecular scattering factors as a function of B . Same test case as in Fig. 8.

molecular models into electron-microscopy reconstructions. The trimeric model was put in a box with cell parameters 418, 342 and 330 Å, which gives 29340 Fourier coefficients. With $R = 1.5$, the grid spacing is now 5 Å. The results for different B factors are shown in Figs. 8 and 9. Equation (29) gives, for $\mathcal{E}^{(\text{theory})} = 10^{-3.5}$, $B = 1875 \text{ \AA}^2$. The average relative error of the calculated Fourier coefficients is 0.0045% and the average phase error is 0.0006° . For the chosen Gaussian cutoff and B factor, atoms contribute up to a radius of 23.7 Å.

6. Conclusions

The numerical results show that structure factors can indeed be calculated by FFT with an acceptable precision using a rather coarse grid – the Lipson & Cochran prescription – up to any desired maximal resolution, provided that appropriate Gaussian cutoff and B dampening factor are used. A point of practical importance is that the value of B is obtained quite simply by solving the analytical expression (29) equated to the desired value of $\mathcal{E}^{(\text{theory})}$.

Anisotropic thermal factors do not complicate the FFT calculations, although the construction of the model electron density becomes more intricate. In this case, the proposed rule to determine the B factor also applies; it suffices to take B_{iso} as corresponding to the smallest sphere inscribed in the thermal ellipsoid.

APPENDIX A

The Fourier transform of a function $\rho(x)$ is defined by

$$f(s) = \int_{-\infty}^{\infty} \rho(x) \exp(2\pi i s x) dx, \quad (32)$$

from which $\rho(x)$ can be recovered by means of the inverse Fourier transform

$$\rho(x) = \int_{-\infty}^{\infty} f(s) \exp(-2\pi i s x) ds. \quad (33)$$

We now divide the x axis into steps of width Δ and compute, instead of the integral (32), the sum

$$c(s) = \Delta \sum_{j=-\infty}^{\infty} \rho(j\Delta) \exp(2\pi i s j \Delta). \quad (34)$$

Replacing $\rho(j\Delta)$ by the Fourier integral (33), and using the expression

$$\sum_{j=-\infty}^{\infty} \exp[2\pi i (u - u') j] = \sum_{n=-\infty}^{\infty} \delta(u - u' + n) \quad (35)$$

of the periodic δ distribution, we obtain

$$\begin{aligned} c(s) &= \Delta \sum_{j=-\infty}^{\infty} \int_{-\infty}^{\infty} f(s') \exp(-2\pi i s' j \Delta) ds' \exp(2\pi i s j \Delta) \\ &= \int_{-\infty}^{\infty} f(s') \sum_{j=-\infty}^{\infty} \exp[2\pi i (s\Delta - s'\Delta) j] d(s'\Delta) \end{aligned}$$

$$\begin{aligned} &= \int_{-\infty}^{\infty} f(s') \sum_{n=-\infty}^{\infty} \delta(s\Delta - s'\Delta + n) d(s'\Delta) \\ &= \sum_{n=-\infty}^{\infty} f(s + n/\Delta). \end{aligned} \quad (36)$$

In three dimensions, we consider the general case of a skew coordinate frame $\{\mathbf{a}_1, \mathbf{a}_2, \mathbf{a}_3\}$ and its associated dual basis $\{\mathbf{a}_1^*, \mathbf{a}_2^*, \mathbf{a}_3^*\}$, which define cells with volumes V and V^{-1} , respectively. Vectors in this space are written in the form

$$\mathbf{r} = \sum_{j=1}^3 x_j \mathbf{a}_j; \quad \mathbf{s} = \sum_{j=1}^3 s_j \mathbf{a}_j^* \quad (37)$$

with coefficients that are dimensionless arbitrary real numbers. Now we have

$$f(s_1, s_2, s_3) = V \iiint_{-\infty}^{\infty} \rho(x_1, x_2, x_3) \exp\left(2\pi i \sum_{j=1}^3 s_j x_j\right) dx_1 dx_2 dx_3 \quad (38)$$

and

$$\begin{aligned} \rho(x_1, x_2, x_3) &= (1/V) \iiint_{-\infty}^{\infty} f(s_1, s_2, s_3) \\ &\quad \times \exp\left(-2\pi i \sum_{j=1}^3 s_j x_j\right) ds_1 ds_2 ds_3. \end{aligned} \quad (39)$$

We divide the $\{x_1, x_2, x_3\}$ axes into steps of widths $\{\Delta_1, \Delta_2, \Delta_3\}$ and compute, instead of the integral (38), the sum

$$\begin{aligned} c(s_1, s_2, s_3) &= V \Delta_1 \Delta_2 \Delta_3 \sum_{j_1, j_2, j_3=-\infty}^{\infty} \rho(j_1 \Delta_1, j_2 \Delta_2, j_3 \Delta_3) \\ &\quad \times \exp\left(2\pi i \sum_{j=1}^3 s_j j_j \Delta_j\right). \end{aligned} \quad (40)$$

Replacing ρ by the Fourier integral (39) and using the definition (35) of the periodic δ distribution, we obtain

$$c(s_1, s_2, s_3) = \sum_{n_1, n_2, n_3=-\infty}^{\infty} f(s_1 + n_1/\Delta_1, s_2 + n_2/\Delta_2, s_3 + n_3/\Delta_3). \quad (41)$$

(j_1, j_2, j_3) and (n_1, n_2, n_3) take integer values.

References

- Brillouin, L. (1956). *Science and Information Theory*, pp. 78–79. New York: Academic Press.
- Doyle, P. A. & Turner, P. S. (1968). *Acta Cryst.* **A24**, 390–397.
- International Tables for X-ray Crystallography* (1992). Vol. C, edited by A. J. C. Wilson. Dordrecht: Kluwer Academic Publishers.
- Lipson, H. & Cochran, W. (1966). *The Determination of Crystal Structures*, 3rd ed., pp. 94–102. Ithaca: Cornell University Press.
- Mathieu, M., Petitpas, I., Navaza, J., Lepault, J., Kohli, E., Pothier, P., Prasad, B. V. V., Cohen, J. & Rey, F. A. (2001). *EMBO J.* **20**, 1485–1497.
- Navaza, J. (1994). *Acta Cryst.* **A50**, 157–163.
- Ten Eyck, L. F. (1977). *Acta Cryst.* **A33**, 486–492.